Ichthyology & Herpetology 113, No. 1, 2025, 44–60

New Species of the Genus *Hypanus* (Dasyatidae) from the Eastern Tropical Pacific Ocean

P. A. Mejía-Falla[1,2], A. F. Navia[2,3], D. Cardeñosa[4], and J. Tavera[5]

A new species of stingray belonging to the genus *Hypanus* is described in this study based on data collected in the Eastern Tropical Pacific (ETP) region of Colombia. This new species stands out within the genus by its unique spade-shaped disc with a width-to-length ratio ranging from 1.0 to 1.1, whereas its obtuse snout extends 29–30% of the disc width (DW). This species also stands out due to its large size (125 cm DW). Notably, it has three distinctive rows of enlarged denticles on its mid-scapular area, with the central row extending back to the caudal sting. Additionally, it possesses a long tail that measures 2.2–2.5 times the DW, tapering smoothly. Molecular data also revealed significant differences between this new species and its congeners using COI. The phylogenetic analysis recovered *Hypanus rubioi*, new species, as the sister species to the western Atlantic Longnose Stingray *H. guttatus*, with an uncorrected genetic distance of 2.27 to 2.94%. The preliminary ecological niche modeling further indicates that this newly described species is likely associated with coastal regions in the ETP, ranging from central Mexico to northern Peru, with backlight and salinity as the most influential variables. These findings contribute to our understanding of the biodiversity within the genus *Hypanus* and the ecological distribution of this novel species in the ETP.

Se describe una nueva raya del género *Hypanus* del Pacífico oriental tropical (POT) a partir de material colectado en el Pacífico de Colombia. La nueva especie es única dentro del género por ser de gran tamaño (125 cm de ancho de disco [AD]) con un disco romboidal en forma de pala, su anchura 1,0 a 1,1 veces su longitud, un hocico obtuso, rostro prolongado de punta extendida, 29–30% en AD, tres filas de dentículos agrandados en la parte media de la escapula, la hilera central se extiende hacia atrás hasta el aguijón caudal, cola larga, 2,2–2,5 veces el AD, estrechándose suavemente. Se diferencia de todos sus congéneres también por diferencias moleculares del gen COI. El análisis filogenético encontró que *Hypanus rubioi* sp. nov. es la especie hermana de la raya laya látigo hocicona del Atlántico occidental *H. guttatus*, con una distancia genética no corregida de (2,27 a 2,94%). El modelado preliminar del nicho ecológico indica además que esta especie recién descrita está probablemente asociada a regiones costeras del POT, que abarcan desde el centro de México hasta el norte de Perú y donde la luz de fondo y la salinidad fueron las variables con mayor influencia en el resultado. Estos resultados contribuyen a nuestra comprensión de la biodiversidad dentro del género *Hypanus* y la distribución ecológica de esta nueva especie en el POT.

THE genus *Hypanus* is composed of ten valid species, one on the west coast of Africa (*Hypanus rudis*), two in the Eastern Tropical Pacific Ocean (ETP; *Hypanus longus* and *H. dipterurus*), and seven in the western Atlantic Ocean (*H. americanus*, *H. berthalutzae*, *H. geijskesi*, *H. guttatus*, *H. marianae*, *H. sabinus*, and *H. say*).

Species of *Hypanus* are broadly distributed along the shorelines of their habitats. *Hypanus americanus* is the most widely distributed species in the Atlantic, ranging from New Jersey (USA) to French Guiana. In contrast, *H. geijskesi* has the most restricted known range in this marine area, found from the Orinoco delta south to Fortaleza in the north of Brazil. In the ETP, the distribution of *H. dipterurus* is greater than that of *H. longus*, going from California to northern Peru (Last et al., 2016). These species exhibit benthic and coastal behaviors, frequently inhabiting sandy bottoms, seagrass beds, lagoons, and reefs, with particularly high abundances in bays and estuaries (Michael, 1993). According to many authors, species of *Hypanus* may have specific habitat requirements, which means that their distribution ranges can be altered by changes in salinity, sea temperature, currents, and other factors (Pyron and Burbrink, 2010; Last et al., 2016; Petean et al., 2020).

Most of these species face high levels of threat from anthropogenic activities such as unsustainable fisheries, habitat degradation, and pollution (Dulvy et al., 2014). Many of these species are regularly caught directly and as bycatch. This is documented in numerous studies for the ETP (López-Garro and Zanella, 2015; Navia and Mejía-Falla, 2016; Morales-Aguilar and Ortiz-Aldana, 2022) as well as in the Caribbean and Atlantic (Mazzoleni and Schwingel, 1999; Costa and Chaves, 2006; Tagliafico et al., 2013; Schmidt et al., 2015; Barrios-Garrido et al., 2017; Hernández-Fernández et al., 2021).

The above-mentioned anthropogenic pressures have led the International Union for the Conservation of Nature (IUCN) Red List of Threatened Species to assess *H. geijskesi* (Pollom et al., 2020a) and *H. rudis* as Critically Endangered (Jabado et al., 2021), *H. marianae* as Endangered (Pollom et al., 2020b), and *H. longus*, *H. dipterurus*, and *H. berthalutzae* as Vulnerable (Pollom et al., 2020c, 2020d; Charvet et al., 2020). The remaining species were considered Near Threatened

[1] Wildlife Conservation Society, WCS Colombia, Av. 5N No. 22N-11, Cali, Colombia.
[2] Fundación Colombiana para la Investigación y Conservación de Tiburones y Rayas, Calle 10 No. 72-35, Cali, Colombia.
[3] Grupo de Investigación en Ecología Animal, Departamento de Biología, Universidad del Valle, Calle 13 No. 100-00, Cali 760032, Colombia.
[4] Department of Biological Sciences, Florida International University, North Miami, Florida.
[5] Grupo de Investigación Sistemática, Evolución y Biogeografía Animal, Instituto de Ciencias del Mar y Limnología, Departamento de Biología, Universidad del Valle, Cali, Colombia; Email: jose.tavera@correounivalle.edu.co. Send correspondence to this address.
Submitted: 5 February 2024. Accepted: 25 October 2024. Associate Editor: M. T. Craig.
 DOI: 10.1643/i2024010 Published online: 18 February 2025

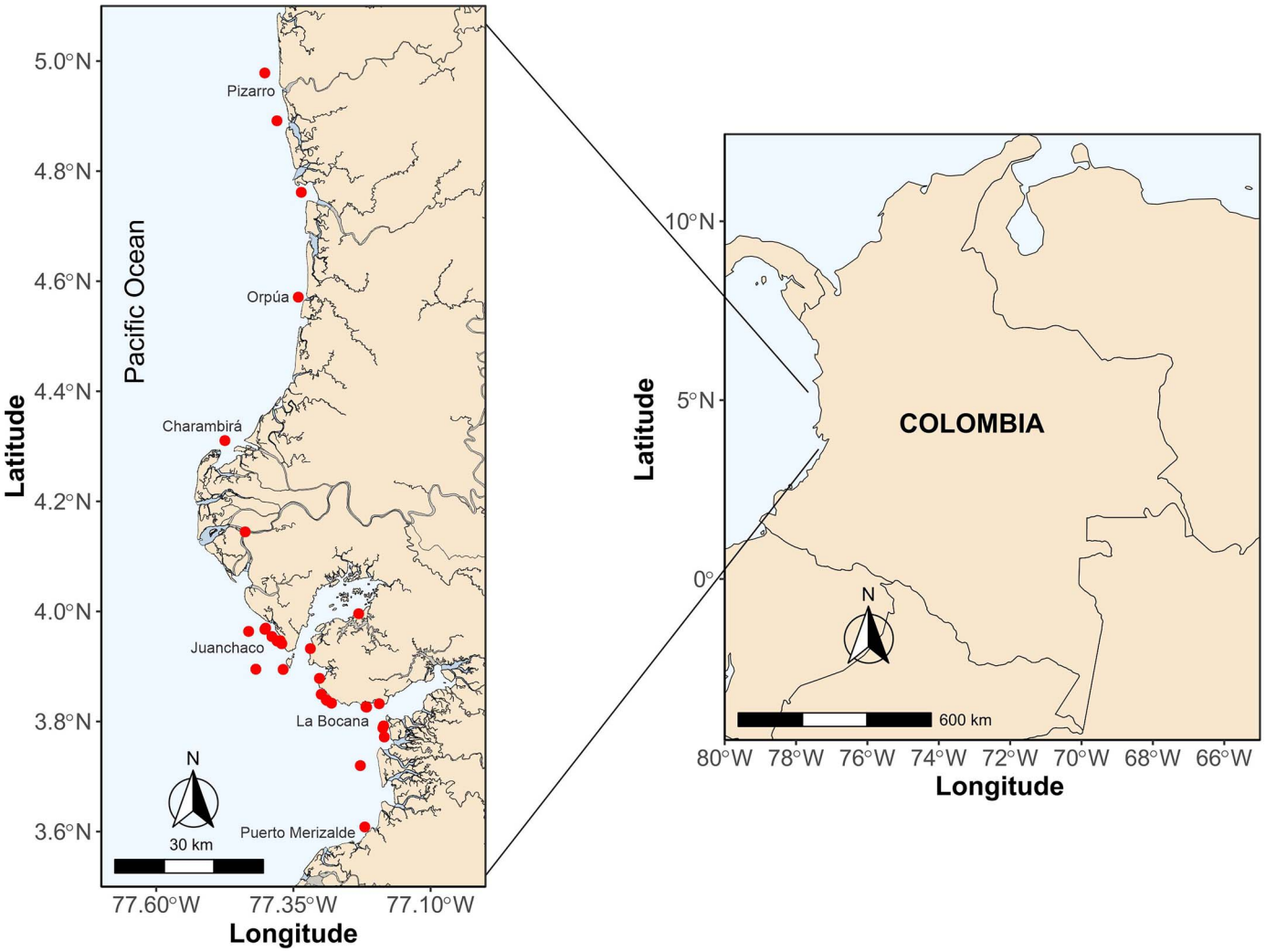

Fig. 1. Distribution of localities where specimens of *Hypanus rubioi*, new species, were collected in the Colombian Pacific Ocean.

(*H. americanus*, *H. guttatus*, and *H. say*) and Least Concern (*H. sabinus*) but with declining population trends (Carlson et al., 2020a, 2020b, 2020c, 2020d).

In the Pacific coast of Colombia, the confirmed presence of *H. longus* and *H. dipterurus* has been previously documented (Mejía-Falla and Navia, 2019). However, since 2003, a species with similar characteristics, but not matching either of these, has been observed. Given that species in *Hypanus* are used as a food source by local fishing communities, the lack of clear taxonomic definition for these species has led to inaccuracies in estimating catches and assessing the risk levels of the genus in the Colombian Pacific coast. Hence, the primary objective of this study is to describe a new ray species found in the Colombian Pacific coast, supported by both anatomical and molecular evidence. Additionally, this study aims to provide preliminary information on the biology, ecology, and potential distribution of this newly described species.

MATERIALS AND METHODS

A total of 90 individuals (47 females, 40 males, 3 unsexed) were detected between 2003 and 2023, during landing and on-board monitoring in artisanal fisheries in the Colombian Pacific, at specific localities between Pizarro, Chocó (4.97833°N, 77.40217°W) and Mallorquín, Valle del Cauca (3.60837°N, 77.21998°W; Fig. 1).

Animals were measured and weighed. The lengths recorded were total length (TL) and disc width (DW) in cm, and total weight in g. Given that this species is primarily used for local consumption or sale, most specimens were unable to be preserved intact upon arrival at port. Instead, they were eviscerated or had their tails removed, thereby precluding their use as reference material. Holotype and additional tissue samples for genetic analysis were collected on a research cruise in the marine-coastal zone of the Uramba Bahía Málaga National Natural Park, Department of Valle del Cauca, within the area of influence of the Juanchaco and Ladrilleros settlements. Additional samples included in this study came from fishing landings off Charambirá, Chocó region, in the northern part of the Colombian Pacific.

Specimens used for description and comparisons were measured following Last et al. (2016) and Manjaji (2004). External morphological descriptions followed Manjaji (2004) and Last and Stevens (2009); clasper descriptions were in accordance with de Moreira et al. (2018). A length–weight relationship was estimated using the power function $TW = a \times S^b$ and the logarithmic form $logTW = loga + b \times logDW$,

where TW is the total weight of the individual, DW is the disc width, *a* is the model intercept, and *b* is the slope. The type of growth (isometric or allometric) was assessed using a student's t test (H0: $b = 3$; Steel and Torrie, 1980). Clasper condition was assessed by considering the degree of calcification and classified as 0 (noncalcified), 1 (partially calcified), or 2 (calcified), with 2 corresponding to mature males (Clark and von Schmidt, 1965; Braccini and Chiaramonte, 2002). Measures of the reproductive structures in males (inner clasper) were plotted against DW to evaluate onset of maturity. Vertebrae were extracted and processed following Mejía-Falla et al. (2014) for a preliminary age estimation of the specimen.

Tissue samples were taken from the pectoral fin of the holotype and one additional specimen (caught and released) stored in 96% ethanol. DNA was extracted following a standard salting-out protocol (Sambrook et al., 1989). PCR amplifications of the mitochondrial gene cytochrome oxidase I (COI) using the FishF1 (5′–TTCTCAACCACA AGACATTGG-3′) and FishR1 (5′–TAGACTTCT GGGGCCAATCA-3′) primers (Ward et al., 2005) were conducted. Amplifications were performed in 13 µl reactions containing 0.5 µl of DNA, 0.625 µl of each primer (forward–reverse), and 11.25 µl of Thermo Scientific 1.1× PCR master mix (2.5 mM $MgCl_2$). After an initial denaturation of 2 min at 95°C, 30–35 cycles at 94°C for 45 seconds (s), followed by 45 s at an annealing temperature of 54°C, and 60 s at 72°C with a final extension of 5 min at 72°C were conducted. Sequencing was performed in one direction on an ABI 3100 automated sequencer (Applied Biosystems, Foster City, CA, USA). COI sequences were available on GenBank for all species of the genus *Hypanus* (only *H. marianae* was unavailable). As generic limits within this family are still uncertain, another member of Dasyatidae, *Pteroplatytrygon violacea*, and a distantly related rhinid, *Rhynchobatus djiddensis*, were used as outgroups for molecular comparisons and a preliminary phylogenetic reconstruction. GenBank accession numbers are as follows: *H. americanus* KT075327, KF461168; *H. berthalutzae* MT326604, MT326605; *H. dipterurus* GU440302; *H. geijskesi* MN105749; *H. guttatus* MN105793, JX034000; *H. longus* MT326628, MT326629; *H. rubioi*, new species, PP133089; *H. rudis* MT326632, MT326634; *H. sabinus* KF461169, JN025277; *H. say* OP056996; *P. violacea* MN105751, MK085554; and *R. djiddensis* JX263419. All COI sequences were cleaned and trimmed with Geneious 9.1.8 (https://www.geneious.com), and Muscle (Edgar, 2004) was used as the alignment algorithm with the default parameters. COI corrected genetic distances were calculated among all taxa included. Phylogenetic relationships were assessed using Bayesian inference. Two independent runs with a random starting tree using GTR+Gamma model of nucleotide substitution were performed with BEAST 2.75 (Bouckaert et al., 2019). Estimated sample sizes, mixture, and convergence of chains were evaluated in Tracer (Rambaut et al., 2018). Tree annotator was used to combine all Bayesian trees into the maximum clade credibility tree, discarding the initial 25% of the trees as the burn in phase.

To estimate the potential distribution area occupied by the species, we used 33 occurrence data points (Supplemental Material, Table 1; see Data Accessibility) applied to a species distribution model (SDM). Based on the known distribution of other species of the family Dasyatidae; the coastal region of the ETP was hypothesized as a possible area M (historically accessible area for the species; Soberón and Peterson, 2005). For model calibration, a 200 km buffer was used according to Barve et al. (2011) and taking as reference the marine ecoregions determined by Spalding et al. (2007). To characterize the species' range, 20 benthic environmental variables from the Bio-Oracle 2.0 repository (Assis et al., 2018) were considered: current velocity, bottom light, primary productivity, salinity, and temperature and for each of them: Lt. min, Lt. max, mean, and range (Lt. refers to the average of the minimum and maximum record per year). Once the environmental variables were obtained, collinearity between them was evaluated to reduce overestimation of the models and bias in statistical inferences (Dormann et al., 2012) by means of a Pearson correlation test with the 'ellipsenm' package (https://github.com/marlonecobos/ellipsenm) in R. Since values greater than 0.7 were considered high collinearity, the variables used were the mean current velocity, bottom light, primary productivity, and temperature, and maximum Lt. of salinity.

The model was built with the Maxent 3.4.3 software (Phillips et al., 2006) using the R package 'KUENM' (Cobos et al., 2019). To determine the appropriate parameterization of the models, the kuenm_cal function was used to test the regularization multipliers between 0.1 and 5 (every 0.5), and the linear 'l,' quadratic 'q,' and hinge 'h' features, with their respective combinations. We used 50% of the data for training and 50% for evaluation, and 10,000 background points were used (Warren and Seifert, 2011; Merow et al., 2013; Cobos et al., 2019). Based on the aforementioned combinations, the evaluation and selection of the best models was performed using the cal_eval function. For this purpose, 1) the statistical significance of the candidate models was evaluated using the average area under the curve (AUC) of the partial receiver operating characteristic (partial ROC), which is based on a traditional ROC (Peterson et al., 2008), with 500 iterations and 50% of the data used for bootstrapping. The AUC varies between 1 and 2, where 1 represents random models and 2 represents better-than-random performance. 2) The models selected in the previous step were evaluated for their performance, selecting only those models whose omission rate was less than 5% (Anderson et al., 2003). 3) The complexity of the previously selected models was assessed, using the Akaike's Corrected AICc (AICc), and retaining those models with AICc values less than 2 (Warren and Seifert, 2011). Subsequently, using the kuenm_mod function, the final models were created using the logistic output (Elith et al., 2011) and ten replicates of the models were created by Bootstrap to add variability to the prediction (Kass et al., 2018; Cobos et al., 2019). In addition, Maxent's jacknife function was used to evaluate the importance of each environmental variable (Phillips et al., 2006). The best candidate models were projected to the previously determined area M using the clamping option (Owens et al., 2013). In order to obtain a single distribution map and uncertainty map, the mean and standard deviation of the final models were calculated with the kuenm_modstats function, and a complementary mobility-oriented parity (MOP) analysis was performed, which measures the distance between the two models (MOP) as the distance between the different points of the calibration area and the projected area, thereby finding the areas of strict extrapolation, which are values that may be outside the range sampled during model training, given some individual variable (Owens et al., 2013).

***Hypanus rubioi*, new species**
urn:lsid:zoobank.org:act:1C4BAFAA-5E61-4830-A88B-8C1620712E96
Longnose Pacific Stingray
Spanish name: Raya picuda
Figures 2, 3, 4

Holotype.—CIRUV 021336, 1,897 mm TL, 608 mm DW, Bahía Málaga, Colombia, 3.96375°N, 77.431583°W, immature male collected with hook and line at 8 m depth, 28 November 2021.

Paratypes.—CIRUV 024008, 1,101.7 mm TL, 326 mm DW, Bahía Málaga, Colombia, 3.96375°N, 77.431583°W, immature male collected with hook and line at 0.5 m depth, 9 December 2021; CIRUV 024073, 504 mm DW, landed in Pueblo Nuevo market, Buenaventura, Colombia, 3.882887°N, 77.075239°W, immature male, without information on location of capture or fishing gear, December 2008; CIRUV 024074, 1,485 mm TL, 405 DW, landed in Pueblo Nuevo market, Buenaventura, Colombia, 3.882887°N, 77.075239°W, female, without information on location of capture or fishing gear, December 2008; CIRUV 024075, 1745 TL, 480 DW, landed in Pueblo Nuevo market, Buenaventura, Colombia, 3.882887°N, 77.075239°W, female without information on location of capture or fishing gear, March 2005.

Diagnosis.—A large-sized species of *Hypanus* (attaining about 1,250 mm DW; Fig. 2) with the following combination of characters: front-side margins of disc concave; snout pointed protruding sharply, rostrum angle 93–105°; disc equal or wider than long, DL 1.0–1.1 times in DW; long slender tail, 2.4 to 3.1 times disk length; tail width 0.6–1.1 times its height, at pelvic fin posterior end; ventral fold low and slender, its length 1.6–2.7 times DW, 13–25 times its depth below pelvic fin posterior end; preoral length 28–32% DW; distance between nostrils 9–11% DW; distance between first gill slits 17–19% DW; distance from anterior cloaca to sting 0.4–0.8 times in precloacal length (Table 1); dorsal surface rough with a row of enlarged denticles, flanked on each side by a short row of irregular mid-scapular blunt thorns; midline denticles extending from behind the head back into the tail to caudal sting.

Hypanus rubioi is distinguished from its two eastern Pacific sympatric species *H. longus* and *H. dipterurus* by having a long (29 to 32% in DW), pointed rostrum compared to 17 to 20% in *H. longus*, and a very long tail (2.4 to 3.1 times its disc length) compared to 2.4 in *H. longus* and 1.2 to 1.6 in *H. dipterurus* (Fig. 3). *Hypanus rubioi* shares with *H. longus* a small ventral caudal fin fold fitting 0.4 to 0.7 times the length of the disc and 0.55 to 0.62 times, respectively, while *H. dipterurus* has a larger fold where its length fits 0.33 times the length of the disc. *Hypanus rubioi* differs from *H. dipterurus* in the number of times the mouth width fits in the preoral length. While in the new species the mouth fits 3.1 to 3.7 times, in *H. dipterurus* it fits only 2.5 to 3 times. The size of the eye also allows separating the species. In *H. rubioi* the eye is smaller (~1.7 to 3.4% of the disc width, while in *H. longus* it is 3.1 to 5.6%). The ratio between internostril width and pre-nasal length is smaller in *H. longus* (1.3–1.8) compared to values of 2.2 to 2.8 times in *H. rubioi*. Finally, the eye of *H. rubioi* fits 4 to 9 times in the interorbital distance, while in *H. longus* it fits 2 to 4 times and in *H. dipterurus* it fits 2.5 times.

Description.—Disc spade-shaped; equal or slightly broader than long, 1.0–1.1 times its length in its width; maximum depth behind spiracles; snout pointed and long; rostrum particularly sharp and pronounced anteriorly; apical lobe acute and triangular; snout angle 93–105°; anterior margin of disc concave, especially closer to the snout; pectoral fin apex rounded; posterior margin convex, increasing toward the rear-most part. Pelvic fins subtriangular, its length from 13 to 18% DW, width 0.6 to 1.1 times in length, slightly convex posterior margin. Clasper rather large, robust, and cylindrical, with significant increase in size from 7% to 15% in DW from juvenile (326 mm DW) to immature males (608 mm DW). Tail long and slender, rounded but tapering toward the end, postcloacal tail 3.0 to 3.4 times precloacal length, tail width 0.6–1.1 times height, at pelvic fin posterior end; sting origin 13.1–16.7% of tail length; surface rough with small blunt thorns and denticles limited to compressed dorsal area reaching but not crossing the sting. Snout long and sharp, preoral length 3.1 to 3.8 times mouth width. Eye diameter 1.8 to 3.4 times in spiracle length. Interorbital distance 11.3–15.5% DW. Spiracles oval, 1.7 to 2.3 times longer than tall. Internasal distance 2.22 to 2.77 times in prenasal distance. Lower jaw subtriangular, symphysial teeth visible ventrally. Gill openings S-shaped, distance between first gill slits 17.8–19.2% DW, distance between the first and the fifth gill slit 1.43 to 1.54 times the distance between first gill slits (Table 1). Dorsal surface covered in rough denticles, becoming progressively sparse toward lateral margin of disc where only a few rows of concentrical denticles remain; behind head a central row of enlarged denticles, flanked on each side by a short row of irregular mid-scapular blunt thorns; this row extends into the tail and ends at caudal sting. Length of sting becoming larger in larger specimens 14% DW in paratype and 25% DW in the holotype (Table 1).

Color in life.—Dorsal surface of disc and tail uniformly brown, with pearl to beige spines and thorns. Ventral area uniformly whitish to pale, with outer margins narrowly dusky, resembling dorsal color. Tail paler near its base but darkening as it moves back to the skin fold (Figs. 2, 3, 4).

Distribution.—*Hypanus rubioi* is found on the shallow shelf of the eastern Pacific coast of Colombia. The known range is between Pizarro, department of Chocó (4.97833°N, 77.40217°W) and Mallorquín, department of Valle del Cauca (3.60837°N, 77.21998°W; Fig. 1), although we suspect this species occurs over a larger range in the ETP. The specimens that were monitored at landings came mainly from the localities of Charambirá (Chocó) and Buenaventura (Valle del Cauca). Fishermen report capturing them exclusively in soft bottom habitats.

Habitat.—Collection depths range from 0.5 to at least 15 m in shallow waters in soft bottoms or mud habitats.

Etymology.—The name *rubioi* comes from the professor Efrain Rubio, who worked for many decades as ichthyology

Fig. 2. Dorsal view of the holotype of *Hypanus rubioi*, new species, CIRUV-021336, male, 1,897 mm disc width, from Bahía Málaga, Colombia.

teacher at Universidad del Valle. Dr. Rubio was one of the first researchers interested in the fish fauna of the Colombian Pacific. During all these years at Universidad del Valle, he started the ichthyology collection (CIRUV) in addition to training many generations of young ichthyologists interested in the Pacific fishes of Colombia.

Bioecology.—Using the 47 females and 40 males recorded in landings and onboard monitoring in artisanal fisheries in the Colombian Pacific, it was found that females presented disc widths between 450 and 1,380 mm (being more frequent between 800 and 900 mm DW; χ = 818 mm DW), while males presented disc widths between 280 and 970

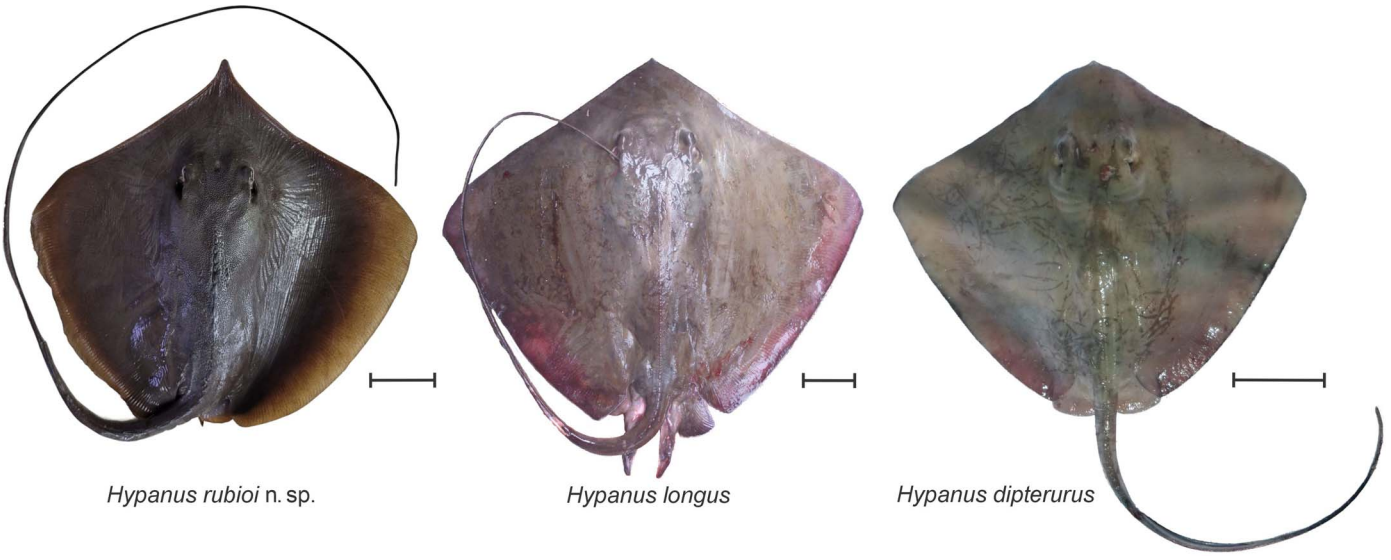

Fig. 3. Comparative morphology of the three sympatric species of the genus *Hypanus* in the Tropical Eastern Pacific. Scale bars = 10 cm.

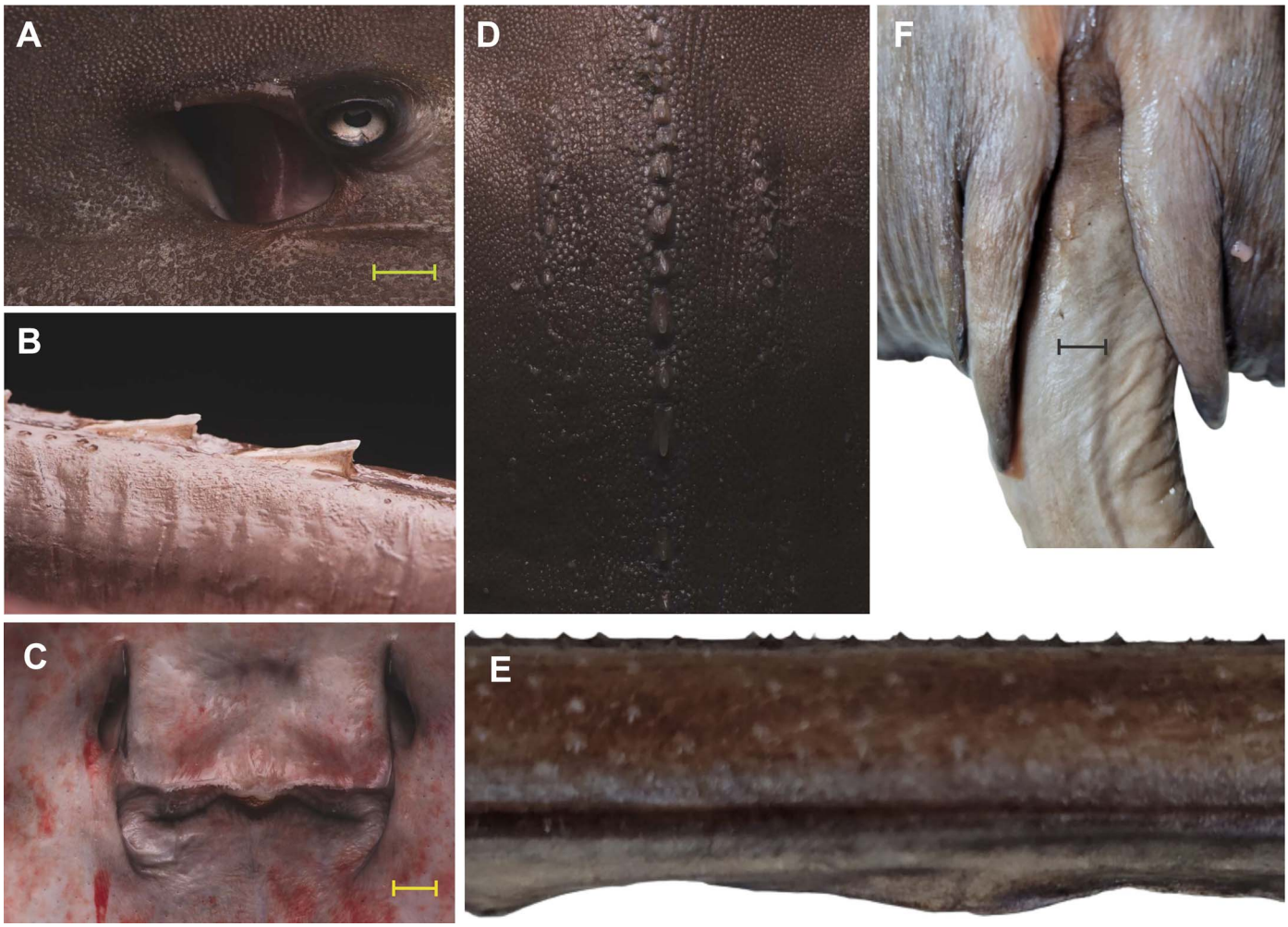

Fig. 4. Body images of holotype of *Hypanus rubioi*, new species, CIRUV-021336. (A) Eye and spiracle, (B) spines of the tail, (C) oronasal region, (D) dorsal thorns, (E) lateral view of the tail, (F) ventral view of claspers. Scale bars = 1 cm.

mm DW with greater representation between 600 and 800 mm DW (χ = 692 mm DW; Fig. 5A). Significant differences in length between sexes were identified (U = 6565; Z = 2.140; *P* = 0.032). For both males and females, high correspondence was observed between disc length and disc width (females y = –3.8568 + 0.9894*x, r^2 = 0.955; males y = 4.0793 + 0.8558*x, r^2 = 0.8180; Fig. 5B). Males considered immature, with uncalcified or partially calcified claspers, presented sizes between 280 and 660 mm DW, while mature males with calcified claspers presented sizes between 660 and 970 mm (Fig. 5C). A 905 mm female, captured in March 2019, was in a pregnant state, with the presence of two pups just beginning their development (not measurable). Vertebral band counts in a 1,040 mm DW specimen suggest an age of at least 7 years (Fig. 5D).

Distribution probability.—Once the presence database was processed, we had a total of 33 georeferenced records of *Hypanus rubioi* located in the central Pacific area of Colombia. A total of 70 candidate models were constructed, all of them with average AUC values greater than 1.9. With respect to the omission rate, 11 models presented values lower than 5%, and of these, only three presented AICc values lower than 2. The three final models were the linear model 'l,' the quadratic model 'q,' and the linear-quadratic model 'lq' with regularization multipliers 0.1, 0.1, and 0.6, respectively. According to the jacknife analysis, the variable with the highest percentage contribution for the three final models was the average value of background light (between 71.1% and 76.0%), followed by the maximum Lt. of salinity (between 9.7% and 10.7%). The variable with the lowest contribution value for the three models was the average current velocity (between 0.5% and 1.0%). The habitat suitability map (Fig. 6) shows that the highest values (estimated area occupied by the species) are closely associated with coastal sections of the ETP (considered as area M), especially some small areas located on the coasts of central México (Fig. 6A), southern México, Guatemala, and El Salvador, and northern Costa Rica (Fig. 6B), and in larger areas along the coasts of Honduras, Nicaragua, and Panamá (Fig. 6C). In addition, habitats with high suitability are found in the central and southern Colombian Pacific (Fig. 6D) and along the entire coast of Ecuador and northern Perú (Fig. 6E). However, it should be noted that the standard deviation map and the MOP analysis show large areas of uncertainty, represented by high values of standard deviation and areas with risk of strict extrapolation, i.e., similarities of 0 or close to 0, so the probability of presence of the species in these areas should be taken with caution (Supplemental Material, Fig. 1; see Data Accessibility).

Table 1. Measurements of five specimens of *Hypanus rubioi*, new species. All measurements are presented in mm.

Measurement	Abbreviation	Holotype CIRUV (021336)	% DW	Paratype CIRUV (024008)	% DW	Paratype CIRUV (024073)	% DW	Paratype CIRUV (024074)	% DW	Paratype CIRUV (024075)	% DW	Average	% DW
Total length	TL	1897		1101.7		—		1485		1745		1557.2	
Angle of the rostrum (°)	AR	105		93		115		100		110		104.6	
Disc width	DW	608.00		326.00		504.00		405.00		480.00		464.60	
Disc length	DL	552.0	90.8	314.0	96.3	495.0	98.2	397.0	98.0	430.0	89.6	437.6	93.8
Mouth to tail	MtT	1,743.0	286.7	1,003.0	307.7	—		1,355.0	334.6	1,605.0	334.4	1,426.5	305.7
Pre-caudal length	PCL	511.0	84.0	282.0	86.5	480.0	95.2	370.0	91.4	440.0	91.7	416.6	89.3
Snout to cloaca length	StC	482.0	79.3	283.0	86.8	372.0	73.8	350.0	86.4	390.0	81.3	375.4	80.5
Cloaca to caudal tip length	CtCT	1,450.0	238.5	919.0	281.9	—		1,085.0	267.9	1,313.0	273.5	1,191.8	255.4
Pre-spine length	PSL	739.0	121.5	416.0	127.6	655.0	130.0	533.0	131.6	605.0	126.0	589.6	126.4
Caudal length	CL	1,375.0	226.2	813.0	249.4	—		1,100.0	271.6	1,327.0	276.5	1,153.8	247.3
Caudal width at spine	CSW	15.4	2.5	7.2	2.2	14.3	2.8	9.3	2.3	13.3	2.8	11.9	2.5
Tail origin to spine origin length	TSL	230.0	37.8	134.0	41.1	190.0	37.7	180.0	44.4	175.0	36.5	181.8	39.0
Caudal width at P2 end	CW	28.8	4.7	13.3	4.1	38.1	7.6	27.7	6.8	29.3	6.1	27.4	5.9
Caudal height at pelvic fin end	CH	24.6	4.0	14.2	4.4	24.3	4.8	21.8	5.4	23.8	5.0	21.7	4.7
Caudal length postventral fold	CLPF	803.0	132.1	551.0	169.0	—		920.0	227.2	1,135.0	236.5	852.3	182.7
Ventral caudal fold height	VFH	5.2	0.8	2.2	0.7	4.7	0.9	2.9	0.7	4.5	0.9	3.9	0.8
Ventral caudal fold length	VFL	350.0	57.6	124.0	38.0	280.0	55.6	230.0	56.8	292.0	60.8	255.2	54.7
Pelvic fin posterior margin	P2PM	78.5	12.9	55.6	17.1	60.0	11.9	65.0	16.0	80.0	16.7	67.8	14.5
Pelvic fin length	P2L	110.1	18.1	59.5	18.2	85.0	16.9	55.0	13.6	82.0	17.1	78.3	16.8
Pelvic fin anterior margin	P2AM	110.3	18.1	63.3	19.4	85.0	16.9	70.0	17.3	90.0	18.8	83.7	17.9
Pelvic fin width	P2W	76.8	12.6	52.8	16.2	55.0	10.9	60.0	14.8	75.0	15.6	63.9	13.7
Clasper internal length	CIL	91.4	15.0	24.3	7.4	50.0	9.9	—		—		55.2	11.8
Clasper external length	CEL	42.5	7.0	7.8	2.4	24.0	4.8	—		—		24.8	5.3
Preorbital length	POBL	186.0	30.6	96.2	29.5	162.0	32.1	122.0	30.1	150.0	31.3	143.2	30.7
Pre-oral length	POL	176.0	28.9	95.9	29.4	155.0	30.8	127.0	31.4	150.0	31.3	140.8	30.2
Pre-nasal length	PNL	142.0	23.4	80.2	24.6	120.0	23.8	102.0	25.2	125.0	26.0	113.8	24.4
Internostril width	INW	58.7	9.6	32.8	10.1	54.0	10.7	37.0	9.1	45.0	9.4	45.5	9.8
Nasal curtain length	NCL	39.0	6.4	16.8	5.2	20.0	4.0	20.0	4.9	25.0	5.2	24.2	5.2
Nasal curtain width	NCW	62.5	10.3	32.5	10.0	48.0	9.5	38.0	9.4	45.0	9.4	45.2	9.7
Mouth width	MW	52.0	8.6	30.5	9.3	44.0	8.7	36.0	8.9	40.0	8.3	40.5	8.7
Mouth length to widest part of disc	MWD	400.0	65.8	220.0	67.5	343.0	68.1	260.0	64.2	335.0	69.8	311.6	66.8
Distance from mouth to base of tail	DMtT	332.0	54.6	184.0	56.4	324.0	64.3	257.0	63.5	285.0	59.4	276.4	59.2
Eye length	EYL	14.5	2.4	10.3	3.2	8.7	1.7	13.9	3.4	14.0	2.9	12.3	2.6
Eye width	EW	9.3	1.5	5.9	1.8	5.3	1.1	6.7	1.6	9.6	2.0	7.4	1.6
Interorbital length	IOL	75.5	12.4	37.0	11.4	78.0	15.5	50.0	12.3	60.0	12.5	60.1	12.9
Interspiracle length	ISL	92.4	15.2	52.9	16.2	80.0	15.9	60.0	14.8	70.0	14.6	71.1	15.2
Spiracle length	SPL	35.0	5.8	20.0	6.1	29.9	5.9	26.0	6.4	28.5	5.9	27.9	6.0
Spiracle width	SW	19.6	3.2	8.6	2.6	17.8	3.5	13.4	3.3	14.8	3.1	14.8	3.2
First gill slit width	1GW	17.1	2.8	7.7	2.3	25.0	5.0	10.0	2.5	12.0	2.5	14.3	3.1

Table 1. Continued.

Measurement	Abbreviation	Holotype CIRUV (021336)	% DW	Paratype CIRUV (024008)	% DW	Paratype CIRUV (024073)	% DW	Paratype CIRUV (024074)	% DW	Paratype CIRUV (024075)	% DW	Average	% DW
Third gill slit width	3GW	20.2	3.3	11.3	3.5	17.0	3.4	9.0	2.2	15.0	3.1	14.5	3.1
Fifth gill slit width	5GW	10.9	1.8	—		18.0	3.6	7.0	1.7	8.0	1.7	11.0	2.4
Distance between first gill slits	DB1GS	108.8	17.9	59.4	18.2	92.0	18.3	77.7	19.2	90.0	18.8	85.6	18.3
Distance between third gill slits	DB3GS	91.2	15.0	54.9	16.9	80.0	15.9	70.0	17.3	75.0	15.6	74.2	15.9
Distance between fifth gill slits	DB5GS	70.7	11.6	40.2	12.3	63.0	12.5	45.0	11.1	60.0	12.5	55.8	12.0
Distance between the first and fifth gill slits	DB1–5GS	70.7	11.6	39.2	12.0	64.0	12.7	50.0	12.3	60.0	12.5	56.8	12.2
Spine length	SL	157.0	25.8	46.7	14.3	—		—		—		—	

Threats.—The species is strongly associated with artisanal fisheries in the southern Colombian Pacific, where all the 90 individuals were recorded in fishing landings. The species is sought after because it provides a good amount of protein per specimen—an adult specimen can weigh more than 25 kg (Fig. 7)—and the liver is also used for medicinal purposes, as is done with many other elasmobranch species (Mejía-Falla et al., 2017; Puentes et al., 2022). The level of threat from fishing is different between the south-central Colombian Pacific zone (mouth of the San Juan River to Tumaco) where rays are frequently consumed, and the northern part of Colombia, where consumption is not as intense. In Charambirá, Chocó, in September 2022, 23 specimens of this species were caught in the same fishing gear. All of these came out alive, and 22 were returned live to the sea (J. Caicedo, pers. comm.). The retained specimen was used for family consumption.

DISCUSSION

The description of a third stingray species in the ETP is of great interest, and its marked morphological differences have surprisingly gone unnoticed. The main differences of this new species include the shape of its disc, which features a pointed, prominent, and concave snout, as well as rounded posterior disc margins, in contrast to the typical rhomboidal discs (Fig. 3). *Hypanus rubioi* is the second largest species of *Hypanus*, reaching a disc width of 125 cm compared to 180 cm for *H. longus* in the ETP (Table 2; Robertson and Allen, 2024). However, the average DW of *H. rubioi* in small-scale fisheries (χ = 78.4 cm DW) is higher than available data for *H. dipterurus* and *H. longus* in Mexico (n = 636, χ = 48.0 cm DW; n = 54, χ = 63.5 cm DW; González-González et al., 2020) and for *H. longus* in Colombia (n = 289, χ = 70.0 cm DW; López-García et al., 2012).

The present study describes this new species, using molecular, morphological, and ecological information for a group of animals that given their large size are difficult to keep in museum fish collections. In Colombia, *H. rubioi* occurs together with both *H. dipterurus* and *H. longus*, but it can be distinguished by its more prominent snout (29–30% DW), an acutely angular (93–105°) tip, and distinctly convex anterior margins. It also features a unique combination of characters: disc width 1.0 to 1.1 times its length, a broad interorbital space 3.2 to 8.9 times orbit length, and a dorsum with three rows of very prominent denticles, with only the central row extending from the back of the head to the sting on the tail. The two lateral rows are short, blunt, and confined to the middle scapula. Its long and slender tail measures 2.2–2.8 times the DW. This new species has probably been misidentified previously with *H. longus* in the past due to similarities in tail size. *Hypanus rubioi* is the third species of the genus *Hypanus* described this century and the first in the ETP. The last species of this taxon described in the region was *H. dipterurus* (Jordan and Gilbert, 1880), nearly a century and a half ago (143 years).

Uncorrected genetic distance based on the 578 bp alignment of the mitochondrial COI between *H. rubioi* and its congeners ranges from 2.27–2.94% (*H. guttatus*) to 14.18% (*H. sabinus*). The greatest intraspecific variation found was that of *H. guttatus* (0.759%), which is even greater than the distance between valid recognized species *H. berthalutzae–H. rudis*, 0.519–0.692%. The

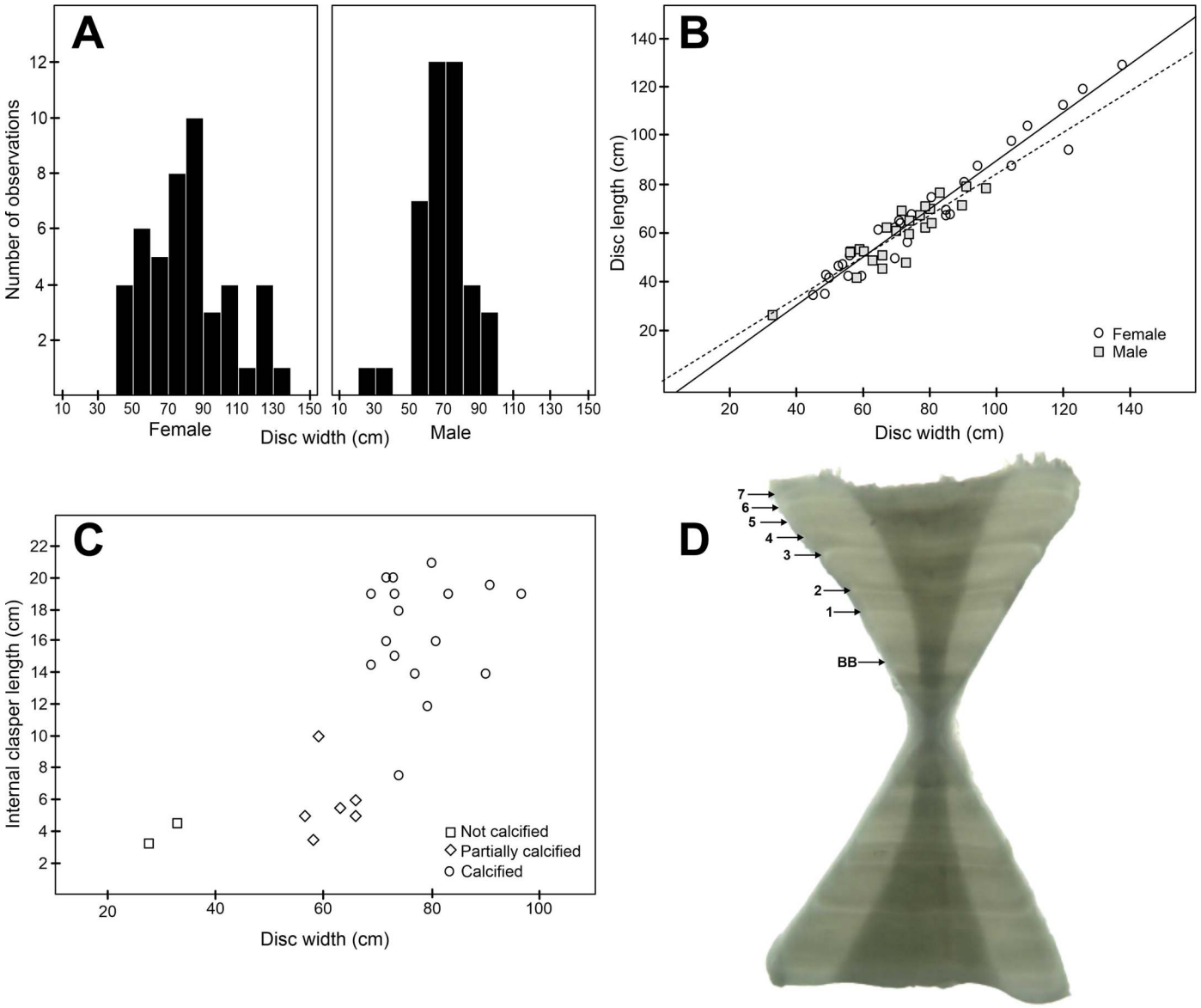

Fig. 5. (A) Distribution of length frequencies of males and females, (B) relationships between disc length and width by sex, (C) maturity stages of males and their relationship with disc width, (D) count of growth bands in a vertebra of a specimen of *Hypanus rubioi*, new species. BB = birth band.

distance of the new species with the Sharpsnout Stingray *H. geijskesi*, recently included in the genus, is around 4.5%. Other elasmobranch species, as those of the genus *Rhizoprionodon* are separated by COI genetic distances of 1.2% to 1.5% (Mendonça et al., 2011), and species from the bonnethead complex *S. tiburo–S. vespertina* ranged from 1.3 to 1.8% (Aroca et al., 2022). Our molecular species separation values are consistent with those found in other stingray groups (Ward et al., 2008). The COI mitochondrial phylogenetic reconstruction (Fig. 8), which includes all valid species of the genus except the Brazilian Large-eyed Stingray *H. marianae*, resulted in a topology with *H. rubioi* nested deep within the genus *Hypanus* and recovered more closely related (posterior probability of 1) to the western Atlantic species *H. guttatus* which it resembles morphologically (Fig. 8). The Sharpsnout Stingray, *H. geijskesi*, was also recovered at the base of this three-species clade of snout-nosed rays. The other two ETP species are allocated in different clades. *Hypanus longus* was recovered sister to the lineage including *H. rudis* + *H. berthalutzae* and *H. americanus*. While *H. dipterurus* is sister to *H. say*, *Hypanus sabinus* was the basal branch of the genus. *Pteroplatytrygon violacea* was nested within the genus *Hypanus*, challenging its monophyly, yet its placement needs to be tested with more data. These results, although robust (all species and most of the clades exhibited 1.0 posterior probability support; Fig. 8), should be treated as preliminary as they are derived exclusively from a single mitochondrial marker.

Hypanus rubioi is commonly captured by artisanal fishermen along the Colombian Pacific coast. Despite Decree 281 of 2021 that prohibits the fishing and commercialization of sharks and rays in Colombia, this and other shark and ray species continue to be caught as bycatch in most of the country's fisheries. As already discussed by Castellanos et al. (2021) and Puentes et al. (2022), the threat status of these species is now even more uncertain since no records of

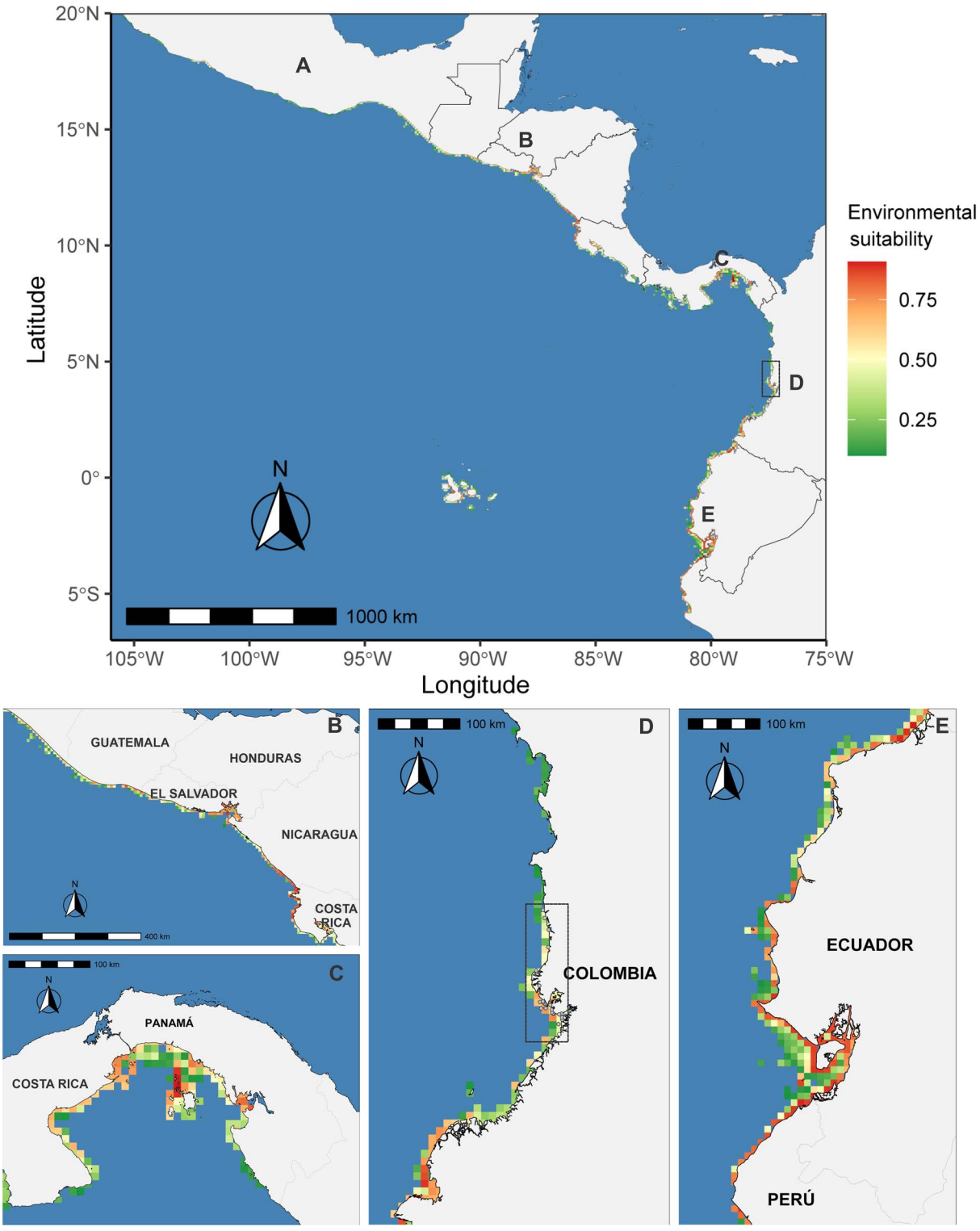

Fig. 6. Environmental suitability map of *Hypanus rubioi*, new species, in the Tropical Eastern Pacific. Coast of central México (A), southern México, Guatemala, El Salvador, Honduras, Nicaragua, and Costa Rica (B), Panamá (C), Colombia (D), and Ecuador and northern Perú (E).

catches are being kept. Fishing communities no longer facilitate the recording of catches of these species, yet they continue to use them. Additionally, it has been documented that since the issuance of the prohibition decree, a black market for shark fins has emerged in the country (Colombian general prosecutor's office, pers. comm.).

Photographic records suggest the presence of *H. rubioi* in Ecuador, although the identity of these specimens must be confirmed (https://www.inaturalist.org/observations/163346941, https://www.inaturalist.org/observations/148447824, https://www.inaturalist.org/observations/108184540, https://www.inaturalist.org/observations/85374335).

Fig. 7. Specimens of *Hypanus rubioi*, new species, caught in artisanal fishing operations in Charambirá, Colombian Pacific Ocean (courtesy of WCS Colombia, Julian Caicedo).

These records would indicate this species is also being caught in artisanal fisheries in the area of the Gulf of Guayaquil, mainly with long-lines. In this regard, Aguilar (2010) recorded 138 specimens (between 2006 to 2007) and identified them as *Dasyatis acutirostra* (now provisionally under *Telatrygon* [Last et al., 2016]), but the image presented in this document looks much more like *H. rubioi* because the rostrum is shorter, 28–32% DW compared to the 37–44% of the Sharpnose Ray, *T. acutirostra*. Furthermore, the natural distribution of *T. acutirostra* (Nishida and Nakaya, 1988) is the northwestern Pacific: China and southern Japan (Nishida and Nakaya, 1990; Fricke et al., 2024), suggesting that the identification of these specimens by

Table 2. Measurements of the five specimens of *Hypanus longus* caught on the Colombian Pacific coast. All measurements are presented in mm.

Measurement	Abbreviation	No. 1	% DW	No. 2	% DW	No. 3	% DW	No. 4	% DW	No. 5	% DW	Average	% DW
Total length	TL	1,000		904		1074		—		—		992.7	
Angle of the rostrum (°)	AR	65		55		52		65		60		59.4	
Disc width	DW	365.0		334.0		400.0		500.0		520.0		423.8	
Disc length	DL	298.0	81.6	290.0	86.8	329.0	82.3	430.0	86.0	435.0	83.7	356.4	84.1
Mouth to tail	MtT	935.0	256.2	825.0	247.0	1,000.0	250.0	—		—		920.0	217.1
Pre-caudal length	PCL	290.0	79.5	280.0	83.8	310.0	77.5	410.0	82.0	400.0	76.9	338.0	79.8
Snout to cloaca length	StC	262.0	71.8	255.0	76.3	280.0	70.0	375.0	75.0	375.0	72.1	309.4	73.0
Cloaca to caudal tip length	CtCT	725.0	198.6	612.0	183.2	750.0	187.5	—		—		695.7	164.1
Pre-spine length	PSL	402.0	110.1	398.0	119.2	440.0	110.0	580.0	116.0	570.0	109.6	478.0	112.8
Caudal length	CL	727.0	199.2	712.0	213.2	770.0	192.5	—		—		736.3	173.7
Caudal width at spine	CSW	8.5	2.3	8.9	2.7	9.5	2.4	10.3	2.1	12.5	2.4	9.9	2.3
Tail origin to spine origin length	TSL	123.0	33.7	112.0	33.5	115.0	28.8	190.0	38.0	165.0	31.7	141.0	33.3
Caudal width at P2 end	CW	19.1	5.2	21.5	6.4	25.1	6.3	25.3	5.1	27.6	5.3	23.7	5.6
Caudal height at pelvic fin end	CH	16.1	4.4	17.4	5.2	18.2	4.6	19.1	3.8	22.3	4.3	18.6	4.4
Caudal length post ventral fold	CLPF	605.0	165.8	533.0	159.6	645.0	161.3	—		—		594.3	140.2
Ventral caudal fold height	VFH	3.6	1.0	2.8	0.8	3.3	0.8	4.9	1.0	5.7	1.1	4.0	1.0
Ventral caudal fold length	VFL	185.0	50.7	175.0	52.4	180.0	45.0	260.0	52.0	250.0	48.1	210.0	49.6
Pelvic fin posterior margin	P2PM	50.0	13.7	35.0	10.5	45.0	11.3	60.0	12.0	77.0	14.8	53.4	12.6
Pelvic fin length	P2L	52.0	14.2	60.0	18.0	60.0	15.0	75.0	15.0	68.0	13.1	63.0	14.9
Pelvic fin anterior margin	P2AM	55.0	15.1	55.0	16.5	60.0	15.0	72.0	14.4	72.0	13.8	62.8	14.8
Pelvic fin width	P2W	50.0	13.7	40.0	12.0	55.0	13.8	55.0	11.0	70.0	13.5	54.0	12.7
Clasper internal length	CIL	30.0	8.2	—		—		44.0	8.8	35.0	6.7	36.3	8.6
Clasper external length	CEL	10.0	2.7	—		—		15.0	3.0	12.0	2.3	12.3	2.9
Preorbital length	POBL	60.0	16.4	65.0	19.5	70.0	17.5	82.0	16.4	85.0	16.3	72.4	17.1
Pre-oral length	POL	70.0	19.2	67.0	20.1	70.0	17.5	97.0	19.4	95.0	18.3	79.8	18.8
Pre-nasal length	PNL	65.0	17.8	46.0	13.8	50.0	12.5	70.0	14.0	70.0	13.5	60.2	14.2
Internostril width	INW	37.8	10.4	33.7	10.1	37.6	9.4	48.7	9.7	50.5	9.7	41.7	9.8
Nasal curtain length	NCL	18.0	4.9	18.0	5.4	20.0	5.0	20.0	4.0	28.0	5.4	20.8	4.9
Nasal curtain width	NCW	34.0	9.3	32.0	9.6	40.0	10.0	45.0	9.0	50.0	9.6	40.2	9.5
Mouth width	MW	24.9	6.8	22.9	6.8	28.3	7.1	32.5	6.5	36.9	7.1	29.1	6.9
Mouth length to widest part of disc	MWD	210.0	57.5	215.0	64.4	245.0	61.3	325.0	65.0	330.0	63.5	265.0	62.5
Distance from mouth to base of tail	DMtT	230.0	63.0	215.0	64.4	240.0	60.0	320.0	64.0	300.0	57.7	261.0	61.6
Eye length	EYL	16.7	4.6	16.7	5.0	22.5	5.6	20.0	4.0	15.9	3.1	18.4	4.3
Eye width	EW	11.0	3.0	9.6	2.9	12.5	3.1	9.9	2.0	10.1	1.9	10.6	2.5
Interorbital length	IOL	49.6	13.6	58.0	17.4	44.1	11.0	68.2	13.6	64.1	12.3	56.8	13.4
Interspiracle length	ISL	53.7	14.7	50.5	15.1	53.6	13.4	69.5	13.9	79.5	15.3	61.3	14.5
Spiracle length	SPL	16.2	4.4	21.8	6.5	19.3	4.8	26.1	5.2	21.8	4.2	21.0	5.0
Spiracle width	SW	11.9	3.3	11.6	3.5	4.9	1.2	16.6	3.3	13.4	2.6	11.7	2.8
First gill slit width	1GW	7.5	2.1	6.4	1.9	8.8	2.2	11.6	2.3	10.2	2.0	8.9	2.1
Third gill slit width	3GW	5.8	1.6	7.4	2.2	10.5	2.6	9.0	1.8	10.0	1.9	8.5	2.0
Fifth gill slit width	5GW	4.4	1.2	5.6	1.7	7.1	1.8	7.2	1.4	8.4	1.6	6.5	1.5
Distance between first gill slits	DB1GS	64.9	17.8	62.3	18.6	67.7	16.9	82.2	16.4	99.9	19.2	75.4	17.8
Distance between third gill slits	DB3GS	56.4	15.4	54.6	16.4	60.3	15.1	74.3	14.9	88.8	17.1	66.9	15.8

Table 2. Continued.

Measurement	Abbreviation	No. 1	% DW	No. 2	% DW	No. 3	% DW	No. 4	% DW	No. 5	% DW	Average	% DW
Distance between fifth gill slits	DB5GS	42.0	11.5	41.3	12.4	51.0	12.8	58.2	11.6	60.5	11.6	50.6	11.9
Distance between the first and fifth gill slits	DB1–5GS	41.6	11.4	40.1	12.0	51.0	12.7	60.9	12.2	63.2	12.2	51.4	12.1
Spine length	SL	—		2.6	0.8	—		—		—		—	

Aguilar (2010) can be misleading. However, Aguilar (2010) indicated that the specimens were frequent in artisanal fisheries landings and had always been important in this activity. This suggests that this species could be facing strong fishing pressure throughout its range, but due to lack of knowledge this has not been evaluated.

The morphometric data used herein to describe *H. rubioi* (five specimens) is limited by sample size given the actual restrictions imposed by the Colombian Decree 281 of 2021. Thus, our data do not fully cover the variability of the species, yet some characters appear to be allometric. Nevertheless, morphology along with molecular (COI) information differed greatly from others in *Hypanus*, including both ETP sympatric species, and are categorical in supporting the new species.

Distribution probability (Ecological niche modeling).—Given that only 33 georeferenced records are available for our analysis, the results of the ecological niche model should still be considered as preliminary and therefore is a first approximation to the knowledge of the ecology and distribution of this species. The current record suggests that the most suitable habitats for *Hypanus rubioi* are those closer to the coast, with backlight and max salinity being the variables that most significantly influence its distribution.

The results of the model suggest that the Gulf of Guayaquil has the highest values of environmental suitability, which is consistent with the record of 138 potential individuals of this species in just one year (Aguilar, 2010). The areas where individuals of *H. rubioi* were recorded in Colombia are mainly estuarine, with a high influence of river mouths and sandy and muddy bottoms, conditions that are also present in the Gulf of Guayaquil (Reynaud et al., 2018). Thus, the presence of the species along the ETP could be expected in areas that share similar conditions to those already described and that the model predicts with greater probability, such as those in southern Colombia, the Gulf of Santa Helena, and Bahía de Salinas in Costa Rica, without restricting itself to these sites. Once new georeferenced records of this species in a wider geographic range become available, this analysis should be updated.

Compared to the latitudinal distribution of *Hypanus dipterurus* (33°N–17°S) and *Hypanus longus* (31°N–3°S) and their respective extents of occurrence, *Hypanus rubioi* is the species with the smallest range of this genus in the ETP. However, it should be considered that the misidentification of specimens, such as the potential case of Ecuador (Aguilar, 2010), substantially reduces the known range, which will be completed as this description helps to clarify the presence of this species in the other countries of the ETP.

DATA ACCESSIBILITY

Supplemental material is available at https://www.ichthyologyandherpetology.org/i2024010. Unless an alternative copyright or statement noting that a figure is reprinted from a previous source is noted in a figure caption, the published images and illustrations in this article are licensed by the American Society of Ichthyologists and Herpetologists for use if the use includes a citation to the original source (American Society of Ichthyologists and Herpetologists, the DOI of the *Ichthyology & Herpetology* article, and any individual image credits listed in the figure aption) in accordance with the Creative Commons Attribution CC BY License. ZooBank

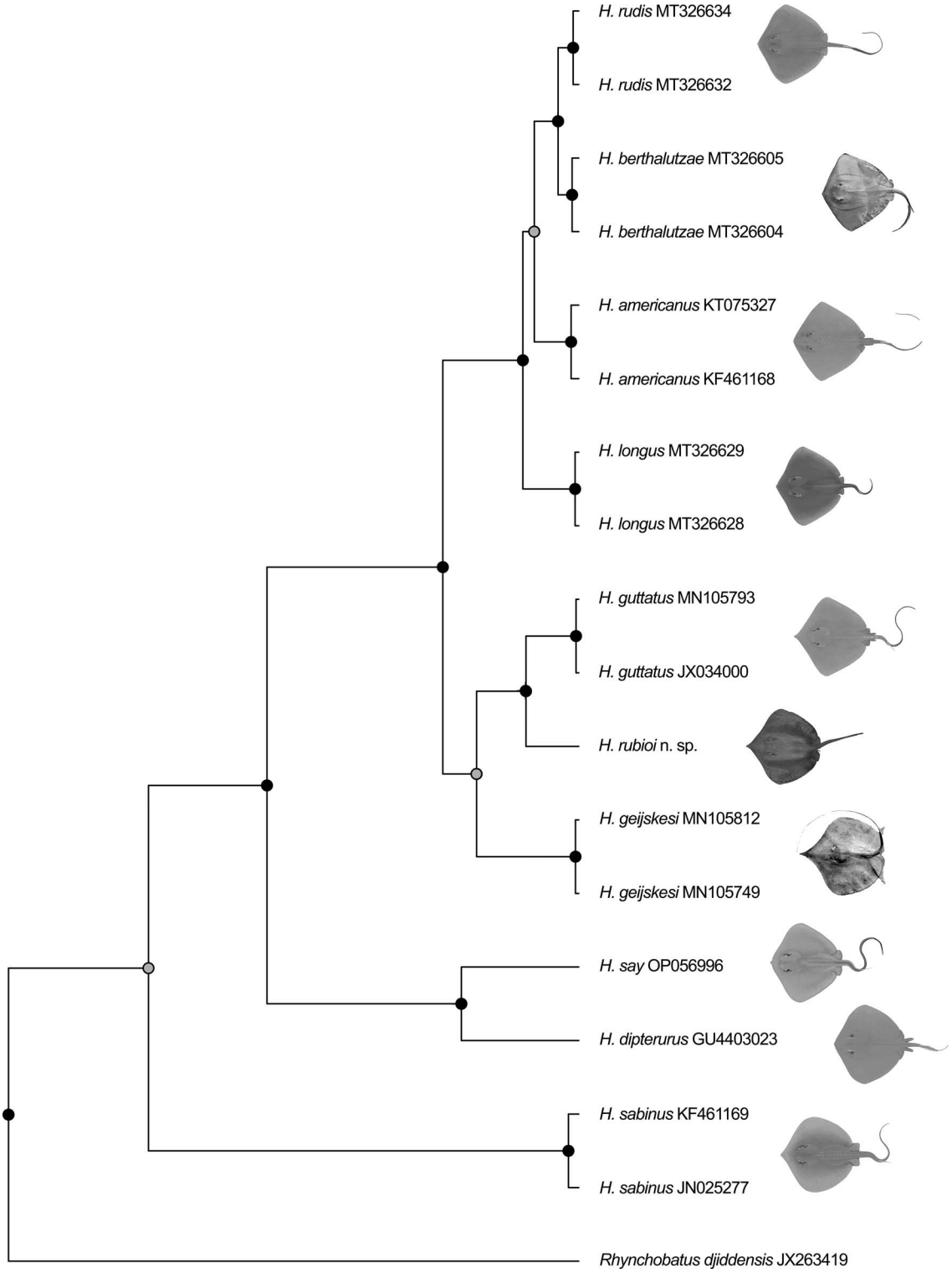

Fig. 8. Bayesian maximum clade credibility COI tree of nine available species of *Hypanus*. Nodes are coded according to posterior probability (pp). Black circles correspond to a support value of 1. Gray circles correspond to 0.75–0.95 pp. White circles indicate 0.75 pp or below. See Data Accessibility for tree file.

publication urn:lsid:zoobank.org:pub:DF0C2E6C-F841-426D-ABE5-1C3A6B6DC9B1.

AI STATEMENT

The authors declare that no AI-assisted technologies were used in the design and generation of this article.

ACKNOWLEDGMENTS

We thank the Afro Community Councils (ACC) of Juanchaco, the ACC of Ladrilleros, the ACC of La Barra, the ACC of Puerto España-Miramar, the ACC of La Plata, and the 22 local traditional knowledgeable people that allowed the development of the Scientific Expedition Pacific 2021-II Bahía Málaga,

Colombian Navy, Colombian Ocean Commission (CCO), Colombia Bio, and the PNNN Uramba-Bahía Málaga. We thank Damian Pardo for all his help during and after the expedition. We thank CCAC Acadesan, Concosta and Río Naya and their fishers, as well as Andes Amazon Fund and Bezos Earth Fund. This is publication number 29 of the Instituto del Mar y Limnología (INCIMAR), Universidad del Valle.

LITERATURE CITED

Aguilar, F. 2010. *Dasyatis acutirostra* (Nashida & Nakaya, 1988) nuevo registro de Raya del género *Dasyatis* en aguas ecuatorianas. Revista de Ciencias del Mar y Limnología, Instituto Nacional de Pesca 4:81–84.

Anderson, R. P., D. Lew, and A. T. Peterson. 2003. Evaluating predictive models of species' distributions: criteria for selecting optimal models. Ecological Modelling 162:211–232.

Aroca, A. K., J. J. Tavera, and Y. Torres. 2022. Molecular and morphological evaluation of the bonnethead shark complex *Sphyrna tiburo* (Carcharhiniformes: Sphyrnidae). Environmental Biology of Fishes 105:1643–1658.

Assis, J., L. Tyberghein, S. Bosch, H. Verbruggen, E. A. Serrão, and O. De Clerck. 2018. Bio-ORACLE v2.0: extending marine data layers for bioclimatic modelling. Global Ecology and Biogeography 27:277–284.

Barrios-Garrido, H., J. Bolivar, L. Benavides, J. Viloria, F. Dugarte, and N. Wildermann. 2017. Evaluación de la pesquería de palangre artesanal y su efecto en la raya látigo (*Dasyatis guttata*) en Isla Zapara, Golfo de Venezuela. Latin American Journal of Aquatic Research 45:302–310.

Barve, N., V. Barve, A. Jiménez-Valverde, A. Lira-Noriega, S. P. Maher, A. T. Peterson, J. Soberón, and F. Villalobos. 2011. The crucial role of the accessible area in ecological niche modeling and species distribution modeling. Ecological Modelling 222:1810–1819.

Bouckaert, R., T. G. Vaughan, J. Barido-Sottani, S. Duchêne, M. Fourment, A. Gavryushkina, J. Heled, G. Jones, D. Kühnert, N. De Maio, M. Matschiner, F. K. Mendes, N. F. Müller, H. A. Ogilvie . . . **A. J. Drummond.** 2019. BEAST 2.5: an advanced software platform for Bayesian evolutionary analysis. PLoS Computational Biology 15:e1006650.

Braccini, J. M., and G. E. Chiaramonte. 2002. Reproductive biology of *Psammobatis extenta*. Journal of Fish Biology 61:272–288.

Carlson, J., P. Charvet, M. P. Blanco-Parra, A. Briones Bell-lloch, D. Cardeñosa, D. Derrick, E. Espinoza, M. Furtado, J. M. Morales-Saldaña, B. Naranjo-Elizondo, N. Pacoureau, R. Rosa, E. V. C. Schneider, and N. J. Simpson. 2020a. *Hypanus sabinus*. The IUCN Red List of Threatened Species 2020:e.T60158A124445557. https://dx.doi.org/10.2305/IUCN.UK.2020-3.RLTS.T60158A124445557.en (accessed 28 August 2023).

Carlson, J., P. Charvet, M. P. Blanco-Parra, A. Briones Bell-lloch, D. Cardeñosa, D. Derrick, E. Espinoza, K. Herman, J. M. Morales-Saldaña, B. Naranjo-Elizondo, N. Pacoureau, E. V. C. Schneider, and N. J. Simpson. 2020b. *Hypanus say*. The IUCN Red List of Threatened Species 2020:e.T60159A3090316. https://dx.doi.org/10.2305/IUCN.UK.2020-3.RLTS.T60159A3090316.en (accessed 28 August 2023).

Carlson, J., P. Charvet, M. P. Blanco-Parra, A. Briones Bell-lloch, D. Cardeñosa, D. Derrick, E. Espinoza, K. Herman, J. M. Morales-Saldaña, B. Naranjo-Elizondo, N. Pacoureau, E. V. C. Schneider, and N. J. Simpson. 2020c. *Hypanus americanus*. The IUCN Red List of Threatened Species 2020:e.T181244884A104123787. https://dx.doi.org/10.2305/IUCN.UK.2020-3.RLTS.T181244884A104123787.en (accessed 28 August 2023).

Carlson, J., P. Charvet, M. P. Blanco-Parra, A. Briones Bell-lloch, D. Cardeñosa, D. Derrick, E. Espinoza, F. Marcante, J. M. Morales-Saldaña, B. Naranjo-Elizondo, E. V. C. Schneider, and J. Simpson. 2020d. *Hypanus guttatus*. The IUCN Red List of Threatened Species 2020:e.T44592A104125629. https://dx.doi.org/10.2305/IUCN.UK.2020-3.RLTS.T44592A104125629.en (accessed 28 August 2023).

Castellanos-Galindo, G. A., P. Herrón, A. F. Navia, and H. Booth. 2021. Shark conservation and blanket bans in the eastern Pacific Ocean. Conservation Science and Practice 3:e428.

Charvet, P., D. Derrick, V. Faria, F. Motta, and N. K. Dulvy. 2020. *Hypanus berthalutzae*. The IUCN Red List of Threatened Species 2020:e.T181244306A181246271. https://dx.doi.org/10.2305/IUCN.UK.2020-3.RLTS.T181244306A181246271.en.

Clark, E., and K. Von Schmidt. 1965. Sharks of the central Gulf coast of Florida. Bulletin of Marine Science 15:13–83.

Cobos, M. E., A. T. Peterson, N. Barve, and L. Osorio-Olvera. 2019. kuenm: an R package for detailed development of ecological niche models using Maxent. PeerJ 7: e6281.

Costa, L., and P. T. C. Chaves. 2006. Elasmobrânquios capturados pela pesca artesanal na costa sul do Paraná e norte de Santa Catarina, Brasil. Biota Neotropica 6(3).

de Moreira, R. A., T. S. Loboda, and M. R. de Carvalho. 2018. Comparative anatomy of the clasper of the subfamily Potamotrygoninae (Chondrichthyes: Myliobatiformes). Journal of Morphology 279:598–608.

Dormann, C. F., S. J. Schymanski, J. Cabral, I. Chuine, C. Graham, F. Hartig, M. Kearney, X. Morin, C. Römermann, B. Schröder, and A. Singer. 2012. Correlation and process in species distribution models: bridging a dichotomy. Journal of Biogeography 39:2119–2131.

Dulvy, N. K., S. L. Fowler, J. A. Musick, R. D. Cavanagh, P. M. Kyne, L. R. Harrison, J. K. Carlson, L. N. K. Davidson, S. V. Fordham, M. P. Francis, C. M. Pollock, C. A. Simpfendorfer, G. H. Burgess, K. E. Carpenter . . . **W. T. White.** 2014. Extinction risk and conservation of the world's sharks and rays. elife 3:e00590.

Edgar, R. C. 2004. MUSCLE: multiple sequence alignment with high accuracy and high throughput. Nucleic Acids Research 32:1792–1797.

Elith, J., S. J. Phillips, T. Hastie, M. Dudík, Y. E. Chee, and C. J. Yates. 2011. A statistical explanation of MaxEnt for ecologists. Diversity and Distributions 17:43–57.

Fricke, R., W. N. Eschmeyer, and R. van der Laan (Eds). 2024. Eschmeyer's Catalog of Fishes: Genera, Species, References. https://researcharchive.calacademy.org/research/ichthyology/catalog/fishcatmain.asp (electronic version accessed 18 May 2024).

González-González, L. D. V., V. H. Cruz-Escalona, N. R. Ehemann, G. D. L. Cruz-Agüero, L. A. Abitia-Cárdenas, P. A. Mejía-Falla, and A. F. Navia. 2020. Richness and

relative abundance of batoids from the artisanal fishery in the Espiritu Santo archipelago, BCS, Mexico. Hidrobiológica 30:37–47.

Hernández-Fernández, G. M., B. Quintana, S. Lara, and F. Santamaria. 2021. Captura de peces elasmobranquios provenientes de la pesca artesanal en las playas de Poneloya y las Peñitas, León, Nicaragua. Revista Iberoamericana de Bioeconomía y Cambio Climático 7:1766–1780.

Jabado, R. W., G. De Bruyne, D. Derrick, P. Doherty, M. Diop, G. H. L. Leurs, K. Metcalfe, G. Porriños, I. Seidu, A. Tamo, W. J. VanderWright, and A. B. William. 2021. *Hypanus rudis*. The IUCN Red List of Threatened Species 2021:e.T161620A124516434. https://dx.doi.org/10.2305/IUCN.UK.2021-2.RLTS.T161620A124516434.en (accessed 28 August 2023).

Jordan, D. S., and C. H. Gilbert. 1880. Notes on a collection of fishes from San Diego, California. Proceedings of the United States National Museum v. 3 (no. 106):23–34.

Kass, J. M., B. Vilela, M. E. Aiello-Lammens, R. Muscarella, C. Merow, and R. P. Anderson. 2018. Wallace: a flexible platform for reproducible modeling of species niches and distributions built for community expansion. Methods in Ecology and Evolution 9:1151–1156.

Last, P. R., G. J. P. Naylor, B. Séret, W. T. White, M. R. de Carvalho, and M. F. W. Stehmann (Eds.). 2016. Rays of the World. CSIRO Publishing, Clayton South, Australia.

Last, P. R., and J. D. Stevens. 2009. Sharks and Rays of Australia. Harvard University Press, Cambridge, Massachusetts.

López-García, J., A. F. Navia, P. A. Mejía-Falla, and E. A. Rubio. 2012. Feeding habits and trophic ecology of *Dasyatis longa* (Elasmobranchii: Myliobatiformes): sexual, temporal and ontogenetic effects. Journal of Fish Biology 80:1563–1579.

López-Garro, A., and I. Zanella. 2015. Capturas de la raya *Dasyatis longa* (Myliobatiformes: Dasyatidae) en las pesquerías artesanales de Golfo Dulce, Costa Rica. Revista de Biología Tropical 63:319–327.

Manjaji, B. M. 2004. Taxonomy and phylogenetic systematics of the Indo-Pacific whip-tailed stingray genus Himantura Muller & Henle 1837 (Chondrichthyes: Myliobatiformes: Dasyatidae). Unpubl. Ph.D. diss., University of Tasmania.

Mazzoleni, R. C., and P. R. Schwingel. 1999. Elasmobranch species landed in Itajaí Harbor, southern Brazil. Notas Técnicas FACIMAR 3:111–118.

Mejía-Falla, P. A., E. Cortés, A. F. Navia, and F. Zapata. 2014. Age and growth of the round stingray *Urotrygon rogersi*, a particularly fast-growing and short-lived elasmobranch. PLoS ONE 9:e96077.

Mejía-Falla, P. A., and A. F. Navia. 2019. Checklist of marine elasmobranchs of Colombia. Universitas Scientiarum 24:241–276.

Mejía-Falla, P. A., A. F. Navia, V. Ramírez-Luna, M. A. Orozco, D. Gómez, D. Amariles, L. A. Muñoz, and K. Torres-Palacios. 2017. Cadena Productiva y Trazabilidad del Recurso Tiburón en Colombia. Informe técnico. Fundación Squalus-AUNAP, Cali, Colombia.

Mendonça, F. F., C. Oliveira, G. Burgess, R. Coelho, A. Piercy, and F. Foresti. 2011. Species delimitation in sharpnose sharks (genus *Rhizoprionodon*) in the western Atlantic Ocean using mitochondrial DNA. Conservation Genetics 12:193–200.

Merow, C., M. J. Smith, and J. A. Silander. 2013. A practical guide to MaxEnt for modeling species' distributions: what it does, and why inputs and settings matter. Ecography 36:1058–1069.

Michael, S. W. 1993. Reef Sharks and Rays of the World. Sea Challengers, Monterey, California.

Morales-Aguilar, J. A., and J. R. Ortiz-Aldana. 2022. Aspectos reproductivos de la raya látigo *Hypanus longus* (Garman, 1880) de los desembarques de la pesca artesanal en el Pacífico de Guatemala. Ciencia, Tecnología y Salud 9:41–54.

Navia, A. F., and P. A. Mejía-Falla. 2016. Fishing effects on elasmobranchs from the Pacific Coast of Colombia. Universitas Scientiarum 21:9–22.

Nishida, K., and K. Nakaya. 1988. A new species of the genus *Dasyatis* (Elasmobranchii: Dasyatididae) from southern Japan and lectotype designation of *D. zugei*. Japanese Journal of Ichthyology 35:115–123.

Nishida, K., and K. Nakaya. 1990. Taxonomy of the genus *Dasyatis* (Elasmobranchia, Dasyatidae) from the North Pacific. *In*: Elasmobranchs as Living Resources: Advances in the Biology, Ecology, Systematics, and the Status of the Fisheries. H. L. Pratt Jr., S. H. Gruber, and T. Taniuchi (eds.). NOAA Technical Report NMFS 90:327–346.

Owens, H. L., L. P. Campbell, L. L. Dornak, E. E. Saupe, N. Barve, J. Soberón, K. Ingenloff, A. Lira-Noriega, C. M. Hensz, C. E. Myers, and A. T. Peterson. 2013. Constraints on interpretation of ecological niche models by limited environmental ranges on calibration areas. Ecological Modelling 263:10–18.

Petean, F. F., G. J. P. Naylor, and S. Q. M. Lima. 2020. Integrative taxonomy identifies a new stingray species of the genus *Hypanus* Rafinesque, 1818 (Dasyatidae, Myliobatiformes), from the Tropical Southwestern Atlantic. Journal of Fish Biology 97:1120–1142.

Peterson, A. T., M. Papeş, and J. Soberón. 2008. Rethinking receiver operating characteristic analysis applications in ecological niche modeling. Ecological Modelling 213:63–72.

Phillips, S. J., R. P. Anderson, and R. E. Schapire. 2006. Maximum entropy modeling of species geographic distributions. Ecological Modelling 190:231–259.

Pollom, R., C. Avalos, J. Bizzarro, M. I. Burgos-Vázquez, A. Cevallos, M. Espinoza, A. González, K. Herman, P. A. Mejía-Falla, J. M. Morales-Saldaña, A. F. Navia, J. C. Pérez-Jiménez, and O. Sosa-Nishizaki. 2020c. *Hypanus longus*. The IUCN Red List of Threatened Species 2020:e.T60157A124445324. https://dx.doi.org/10.2305/IUCN.UK.2020-3.RLTS.T60157A124445324.en (accessed 28 August 2023).

Pollom, R., R. Barreto, P. Charvet, V. Faria, K. Herman, F. Marcante, and G. Rincon. 2020b. *Hypanus marianae*. The IUCN Red List of Threatened Species 2020:e.T45925A104130004. https://dx.doi.org/10.2305/IUCN.UK.2020-3.RLTS.T45925A104130004.en (accessed 28 August 2023).

Pollom, R., J. Bizzarro, M. I. Burgos-Vázquez, A. Cevallos, X. Vélez-Zuazo, C. Avalos, M. Espinoza, A. González, K. Herman, P. A. Mejía-Falla, A. F. Navia, J. C. Pérez-Jiménez, and O. Sosa-Nishizaki. 2020d. *Hypanus dipterurus*. The IUCN Red List of Threatened Species 2020:e.T60152A80677563. https://dx.doi.org/10.2305/IUCN.UK.2020-3.RLTS.T60152A80677563.en (accessed 28 August 2023).

Pollom, R., P. Charvet, V. Faria, K. Herman, O. Lasso-Alcalá, F. Marcante, J. Nunes, and G. Rincon. 2020a.

Fontitrygon geijskesi. The IUCN Red List of Threatened Species 2020:e.T60153A104172152. https://dx.doi.org/10.2305/IUCN.UK.2020-3.RLTS.T6015.en (accessed 4 June 2024).

Puentes, V., P. A. Mejía-Falla, J. G. Ramirez, L. M. Manjarrés-Martínez, J. M. Rguez-Baron, L. A. Zapata, and A. F. Navia. 2022. Sharks and marine batoids management in Colombia: policy instruments, management duty and implications for their populations and stakeholders. Marine Policy 145:105264.

Pyron, R. A., and F. T. Burbrink. 2010. Hard and soft allopatry: physically and ecologically mediated modes of geographic speciation. Journal of Biogeography 37:2005–2015.

Rambaut, A., A. J. Drummond, D. Xie, G. Baele, and M. A. Suchard. 2018. Posterior summarization in Bayesian phylogenetics using Tracer 1.7. Systematic Biology 67:901–904.

Reynaud, J. Y., C. Witt, A. Pazmiño, and S. Gilces. 2018. Tide-dominated deltas in active margin basins: insights from the Guayas estuary, Gulf of Guayaquil, Ecuador. Marine Geology 403:165–178.

Robertson, D. R., and G. R. Allen. 2024. Shorefishes of the Tropical Eastern Pacific: online information system. Version 3.0. Smithsonian Tropical Research Institute, Balboa, Panamá (accessed 28 May 2024).

Sambrook, J., E. R. Fritsch, and T. Maniatis. 1989. Molecular Cloning: A Laboratory Manual. Second edition. Cold Spring Harbor Laboratory Press, Cold Spring Harbor, New York.

Schmidt, B. F., A. F. Amorim, and A. W. S. Hilsdorf. 2015. PCR–RFLP analysis to identify four ray species of the genus *Dasyatis* (Elasmobranchii, Dasyatidae) fished along the southeastern and southern coast of Brazil. Fisheries Research 167:71–74.

Soberón, J., and A. T. Peterson. 2005. Interpretation of models of fundamental ecological niches and species' distributional areas. Biodiversity Informatics 2:1–10.

Spalding, M. D., H. E. Fox, G. R. Allen, N. Davidson, Z. A. Ferdaña, M. A. X. Finlayson, and J. Robertson. 2007. Marine ecoregions of the world: a bioregionalization of coastal and shelf areas. BioScience 57:573–583.

Steel, R. G. D., and J. H. Torrie. 1980. Principles and Procedures of Statistics: A Biometrical Approach. McGraw-Hill, New York.

Tagliafico, A., N. Rago, and M. Salomé Rangel. 2013. Aspectos biológicos de las rayas *Dasyatis guttata* y *Dasyatis americana* (Myliobatiformes: Dasyatidae) capturadas por la pesquería artesanal de la isla de Margarita, Venezuela. Revista de Biología Marina y Oceanografía 48:365–373.

Ward, R. D., B. H. Holmes, W. T. White, and P. R. Last. 2008. DNA barcoding Australasian chondrichthyans: results and potential uses in conservation. Marine and Freshwater Research 59:57–71.

Ward, R. D, T. S. Zemlak, B. H. Innes, P. R. Last, and P. D. N. Hebert. 2005. DNA barcoding Australia's fish species. Philosophical Transactions Royal Society B 360:1847–1857.

Warren, D. L., and S. N. Seifert. 2011. Ecological niche modeling in Maxent: the importance of model complexity and the performance of model selection criteria. Ecological Applications 21:335–342.